

WIND EFFECTS AND CABLES DAMPING AT THE ADIGE CABLE STAY BRIDGE

Massimo MAJOWIECKI
Associate Professor
University IUAV Venezia
Venezia, ITALY

Nicola Cosentino
PhD Structural Engineer
Engineering Consulting
Bologna, ITALY

Carlotta Costa
PhD Structural Engineer
Engineering Consulting
Firenze, ITALY

Summary

The goal of this paper is to restore a design experience, concerning the main aeroelastic problems of cable stayed bridges, as carried out for the new bridge across the Adige river. The first task concerns the aeroelastic excitation of the bridge deck, that is the flutter instability and the vortex shedding excitation. The second one considers the suppression or, at least, the mitigation of the stays vibration mainly due to wind and rain-wind excitation.

The deck aeroelastic stability is evaluated, based on aeroelastic tests carried out at the Politecnico of Milano wind tunnel. The tests, on a 1:30 scaled deck model, consisted in measuring the aeroelastic derivatives in both free and forced motion. The flutter critical conditions (velocity and frequency) are calculated by mean of the Scanlan-Tomko procedure and compared with the simplified Theodorsen theory. The influence of the angle of attack and of the inherent structural damping on the critical parameters has been outlined. Results substantially show that the bridge deck does not suffer flutter instability.

The cable vibration mitigation has been faced by mean of classical viscous dampers. Despite the simplicity of the technical solution, different practical design problems arise. In the paper, a particular attention is reserved to the optimization criteria for the evaluation of the damping coefficients and to the determination of the energy, which has to be dissipated by the dampers.

Keywords: cable stayed bridges; wind induced vibration; flutter; vortex shedding; cable damping; non-classical damping; damping optimization.

1. Introduction

The present paper reports two basic experiences related to the design of a cable stayed bridge (across the Adige River): the aeroelastic excitation of the bridge deck and the cable vibration mitigation.

Regarding the first task, the attention has been focused on the flutter instability and on the vortex shedding excitation; the problem has been experimentally faced, by determining the aeroelastic parameters in wind tunnel tests carried out at the Politecnico of Milano boundary layer wind tunnel. The flutter critical conditions are determined in terms of critical velocity and frequency; the bridge dynamic behaviour is approximated by a 2 DOFs sectional model of the deck; aerodynamic properties of the deck are resumed by the experimentally determined aerodynamic force coefficients and the aeroelastic derivatives. The knowledge of the aeroelastic derivatives and, in particular, their values at very low reduced velocity, allow to evaluate (at least as order of magnitude) the sensibility of the bridge deck to be excited by the vortex shedding phenomenon. As a matter of fact, the wind tunnel investigation has considered the tower aerodynamic and aeroelastic behaviour, too. Nevertheless, due to space limitations, this aspect is not treated in the present paper.

The second aspect which is treated in the paper concerns the damping of cable against dynamic excitations. It is well known that one of the main stay problems is the susceptibility to be dynamically excited. This is due to both the wide range of external load frequencies (wind action, pedestrian and vehicular dynamic loads, decks or towers movement, etc.) and to the very small inherent damping in highly tensioned cables (usually lower than 1‰). In addition, in the present case study, the stay dimensions (length and diameter) are among the most sensitive to rain-wind induced vibrations. The induced vibrations, if they are not suppressed or strongly mitigated, can give rise to fatigue problems and damages in cables and/or anchorage systems. In this paper, the typical design problems in determining the damper characteristics are discussed with reference to the Adige bridge case.

2. Bridge deck aeroelastic behaviour

The bridge deck section (Figure 1) is studied as a rigid mechanical system, characterised by a deck width B , a deck thickness D and a bridge main span length L . The equations of motion, which describe the dynamic system unit length, can be written as:

$$\begin{cases} m\ddot{y} + c_y\dot{y} + k_y y = F_Y \\ I\ddot{\alpha} + c_\alpha\dot{\alpha} + k_\alpha \alpha = M_Z \end{cases} \quad (1)$$

where m is mass and I is the mass momentum of inertia.

Resulting wind forces, acting on the section, can be decomposed into a lift force F_L , a drag force F_D and an aerodynamic moment M_a , applied on the center of mass G . Vertical force F_Y is obtained combining lift and drag forces; with reference to the global coordinate system:

$$F_Y = -F_L \cos \alpha + F_D \sin \alpha \quad (2)$$

Linearized theory is adopted, that is the angle of attack, that is the angle between the section chord and the main flow direction, is supposed to be sufficiently small. This allows one to assume that $|F_Y| = |F_L|$.

Referring to Figure 2, the bridge stiffness properties are resumed by vertical and torsional springs, k_Y and k_α , while the damping properties are considered by mean of the damping coefficients c_Y and c_α . The elastic center E corresponds to the application point of dampers and springs and, in force of the assumed symmetry of the section, it coincides with the center of mass G . They are both located at the midspan of the section.

The section has 2 DOFs, vertical and torsional, around the elastic center. Two reference systems are defined: a cartesian inertial reference frame $OXYZ$ and a joint to the vibrating structure coordinate system $Gx'y'z'$, with the origin coincident with centre of mass G and x' and y' axes oriented, respectively, along the sectional middle line chord and the orthogonal direction.

The angle between the two systems coincides with the angle of attack, which defines the position of the section with respect to the mean wind direction, assumed to be coincident with the X direction.

2.1 The bridge deck section loading model

If the superposition principle is assumed to be applicable, the sectional time-varying wind load can be expressed as the sum of a quasi-steady component, a buffeting fraction, a vortex-shedding induced one and a self-excited one, directed along the global reference axes. In studying the aeroelastic behavior of the bridge deck section, the main attention is focused on the aeroelastic instability due to flutter; hence, the self-excited forces have to be defined.

The most common expression for sectional self-excited forces is in the mixed time-frequency domain; the self-excited forces are modeled by means of parameters (aeroelastic derivatives) which are functions of the frequency response.

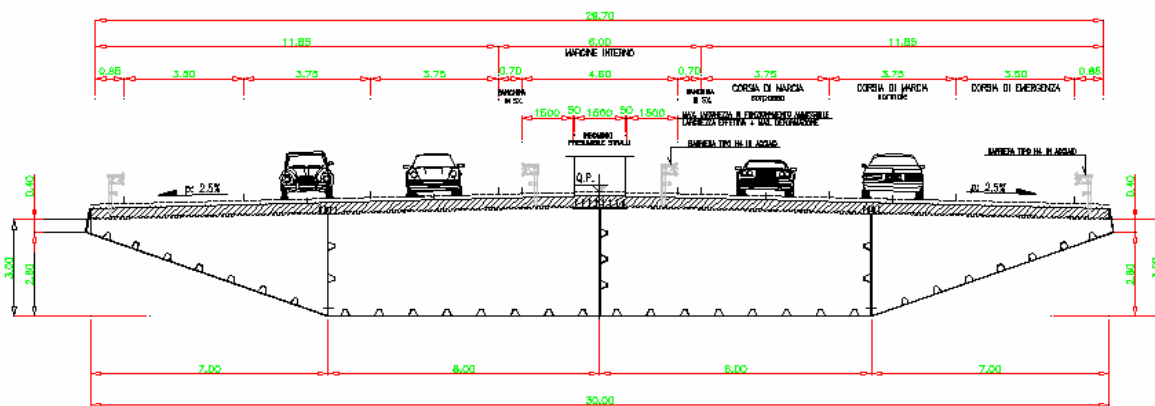


Figure 1. Adige bridge deck section.

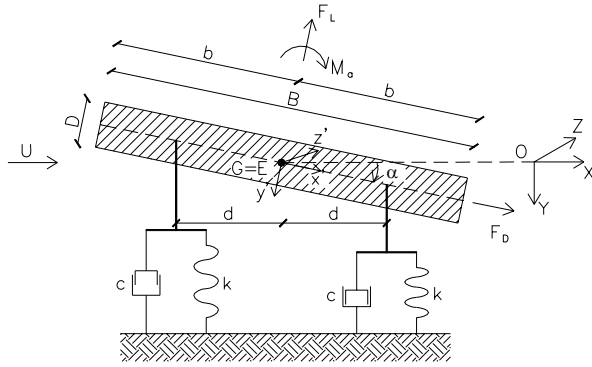


Figure 2. Numerical model of the bridge deck section.

This formulation is due to Scanlan and Tomko [1] and is based on a sinusoidal coupled motion of a 2 DOFs sectional model, with a reduced frequency $K = \omega B/U$:

$$\begin{aligned} F_L(t) &= qB \left[KH_1^*(K) \frac{\dot{y}(t)}{U} + KH_2^*(K) \frac{B\dot{\alpha}(t)}{U} + K^2 H_3^*(K) \alpha(t) + K^2 H_4^*(K) \frac{y(t)}{U} \right] \\ M_a(t) &= qB^2 \left[KA_1^*(K) \frac{\dot{y}(t)}{U} + KA_2^*(K) \frac{B\dot{\alpha}(t)}{U} + K^2 A_3^*(K) \alpha(t) + K^2 A_4^*(K) \frac{y(t)}{U} \right] \end{aligned} \quad (3)$$

where ρ is the air density, $q=1/2 \rho U^2$ is the kinetic pressure, H_i^* and A_i^* ($i=1, \dots, 4$) are the aeroelastic derivatives, commonly identified in wind tunnel tests as function of the reduced frequency K or the reduced velocity $U_{red} = 2\pi / K = 2\pi U / \omega B$.

In the present case, the aeroelastic derivatives have been determined at the Politecnico di Milano wind tunnel [2]. The measured values of the most significant flutter derivatives, H_1^* and A_2^* , are plotted in Figure 3.

In order to keep the aeroelastic behaviour at very low wind speeds, an alternative approach to the flutter problem has been adopted [3]. By this approach, the Equations (3) become:

$$\begin{aligned} F_L(t) &= qB \left(h_1^* \frac{\dot{y}}{U} \quad h_2^* \frac{B\dot{\alpha}}{U} + h_3^* \alpha + h_4^* \frac{\pi}{2V_\omega^2} \frac{y}{B} \right) \\ M_a(t) &= qB^2 \left(a_1^* \frac{\dot{y}}{U} \quad a_2^* \frac{B\dot{\alpha}}{U} + a_3^* \alpha + a_4^* \frac{\pi}{2V_\omega^2} \frac{y}{B} \right) \end{aligned} \quad (4)$$

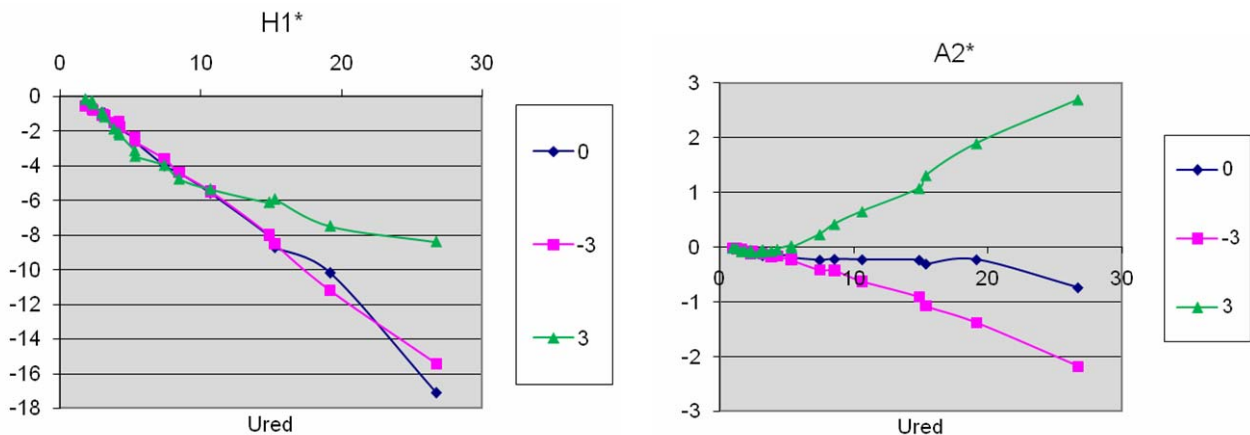


Figure 3. Flutter derivatives H_1^* and A_2^* , measured at the Politecnico di Milano wind tunnel for the attack angles 0° , 3° , -3° .

where the relationships among aeroelastic parameters are:

$$H_1^* = -\frac{h_1^*}{K}; H_2^* = \frac{h_2^*}{K}; H_3^* = -\frac{h_3^*}{K^2}; H_4^* = \frac{\pi}{2} h_4^*; A_1^* = \frac{a_1^*}{K}; A_2^* = -\frac{a_2^*}{K}; A_3^* = -\frac{a_3^*}{K}; A_4^* = -\frac{\pi}{2} a_4^*. \quad (5)$$

2.2 Flutter equation solution

The self-excited forces depend on the motion of the system: the study of the aeroelastic two-dimensional system is more complex with respect to the quasi-steady regime, because of the dependency on the reduced frequency K . Nevertheless, it is possible to identify critical flutter condition, if flutter derivatives are known, by mean of the following procedure which involves the solution of an eigenvalue problem.

In fact, if the motion of the system is harmonic with circular frequency ω , non-trivial solution of the eigenvalue problem can be searched by setting to zero the matrix coefficients determinant. A fourth-degrees complex equation is obtained. If real and imaginary parts are splitted, two real equations are obtained. Solutions for the two real equations are searched, by varying the reduced frequency K : the point (Kc, Xc) , which represents the common solution of the two equations, identifies flutter condition. Finally, incoming wind speed U_{crit} , corresponding to the unstable system, can be obtained. Typical diagrams to obtain critical conditions are shown in Figure 4, where the solution of the flutter equations are referred to the coupling of the first and the third vibration modes and to an angle of attack of 0° .

The two plots of Figure 4 are referred to different interpolation methods for the experimental coefficients: with a linear function in the first case (on the left); with a third degree polynomial function in the second case (on the right). It is interesting to observe that the two different solutions are approximately coincident, if experimental approximation in determining flutter coefficients is taken into account.

In order to calculate flutter velocity, all the flutter coefficients have to be known at the different reduced frequencies; the ratio between the vertical and the torsional frequency of the bridge deck has to be known also. For this reason, it is common to extract flutter derivatives for bridge decks in wind tunnel, being not available analytical expression valid for different geometries. Theoretical expressions are only available for flat plate; they where determined by Theodorsen (1935) for a thin airfoil, with the use of a special function called the circulation function. As a matter of fact, a hybrid method can be used as useful reference tool, by assuming that the bridge deck section is sufficiently streamlined, applying elastic and inertial parameters of the real deck and flutter derivative corresponding to flat plate.

Main results of the described procedures, applied to the Adige Bridge, are reported in the following; the effect of the angle of attack on the flutter wind speed is also outlined. Since the above cited tool is valid for a two-dimensional scheme, the modal analysis of the entire bridge is necessary to identify the natural frequencies and the modal shapes which are susceptible to coupling phenomena and subsequent flutter excitation; main results are synthesized in Table 2, while Table 1 resumes the geometrical and the inertial parameters.

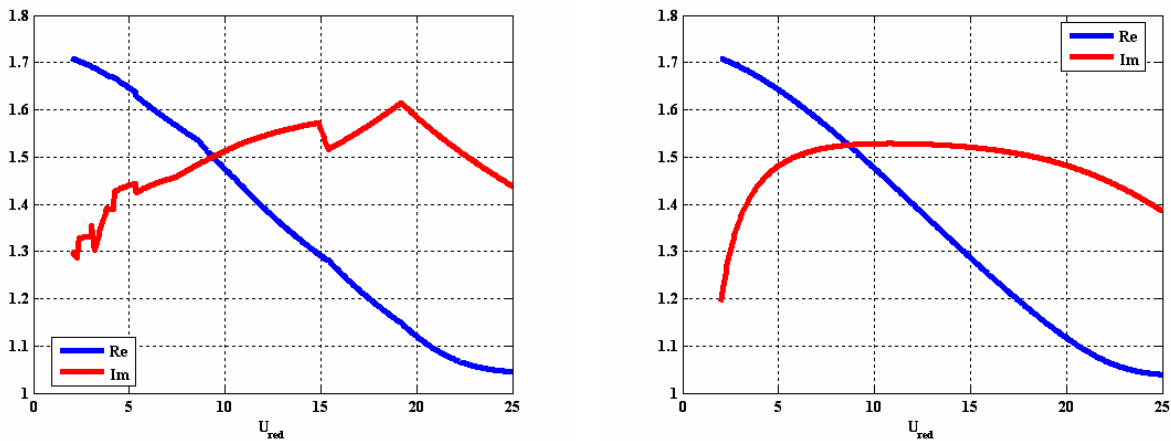


Figure 4. Real and imaginary parts of the flutter equation solution. Coupling of modes 1 and 3 – angle of attack 0° - linear interpolation vs polynomial fitting of experimental coefficients.

Table 1. Geometrical and inertial parameters of the Adige bridge deck section.

L [m]	b [m]	D [m]	B [m]	m [kgm ⁻¹]	I [kgm]
1.0	15.0	3.9	30.0	46500	3400000

Table 2. Modal analysis results (V=vertical; T=torsional; S=symmetric; A=non-symmetric).

Mode #	ω^2 [rad/sec] ²	ω [rad/sec]	f [Hz]	Modal mass	Shape type
1	6.9255	2.632	0.42	8484.1	VS
2	14.3219	3.784	0.60	8364.3	VA
3	20.4147	4.518	0.72	7114.4	TS
11	81.2181	9.012	1.43	6998.9	TA

Table 3. Critical flutter wind speed and frequencies for different angles of attack and damping values.

Modes	ξ [%]	Flat plate		$\alpha = -3^\circ$		$\alpha = 0^\circ$		$\alpha = 3^\circ$	
		U_{crit} [m/s]	f_{crit} [Hz]	U_{crit} [m/s]	f_{crit} [Hz]	U_{crit} [m/s]	f_{crit} [Hz]	U_{crit} [m/s]	f_{crit} [Hz]
1+3	0	220	0.54	218	0.56	166	0.64	70	0.70
1+3	0.5	223	0.53	223	0.55	185	0.62	86	0.69
2+11	0	486	0.93	484	1.02	366	1.23	140	1.40
2+11	0.5	490	0.92	494	1.00	406	1.19	174	1.38

For the present case study, three sets of flutter coefficients are experimentally available and are here considered, respectively for the angles of attack 0° , -3° and 3° . Different modes coupling have been evaluated; the most prone to flutter excitation are the mode couples 1-3 and 2-11. Two different structural damping ratio have been hypothesized, that is $\xi_i = 0\%$ and $\xi_i = 0.5\%$ for all the considered modes. Table 3 resumes the main result of the study.

The critical flutter speed is equal to 70 m/s in the worst case of coupling between first and third modes, under the angle of attack $+3^\circ$ and zero structural damping; such a critical value increases up to 86 m/s if an even very small structural damping is considered. It is interesting to observe the similitude of the theoretical flat plate model and the experimental model at $\alpha = -3^\circ$.

It seems important to observe that accounting for large angle of attack ($\pm 3^\circ$, in this case) is particularly safety. Therefore, flutter does not seem to be a relevant problem for the studied structure. Nevertheless, it is interesting to evidence the sensitivity of this structure to the angle of attack: critical flutter frequency and critical wind velocity evidence a very strong variation, with the increase of the angle of attack. The type of instability changes also, because it varies from a coupled flutter to a purely torsional flutter instability (very dangerous for the structure). Therefore, in order to cover the different working conditions for the structure, wind tunnel tests have to be carried out for different angles of attack.

3. Bridge deck vortex shedding

Wind tunnel tests performed at low wind speeds have evidenced negative values of h_1^* and a_2^* (Figure 5), that is index of a possible interaction between vortex-shedding and structural motion (lock-in).

The main parameter to define the sensitivity of the structure to the vortex shedding is the Scruton number defined as

$$S_{cr} = \frac{\xi m}{\rho D^2} \quad (6)$$

In the case of the Adige Bridge, even if a small value is hypothesized for the damping ratios $\xi_i = 0.5\%$, the Scruton number assumes values which are higher than 10 (~ 14), that is vortex shedding phenomenon should not be afraid.

On the other hand, if the aeroelastic problem is accounted for, it is possible to calculate the minimum damping necessary to avoid the excitation due to vortex shedding. By considering the only equation of motion for the vertical displacement,

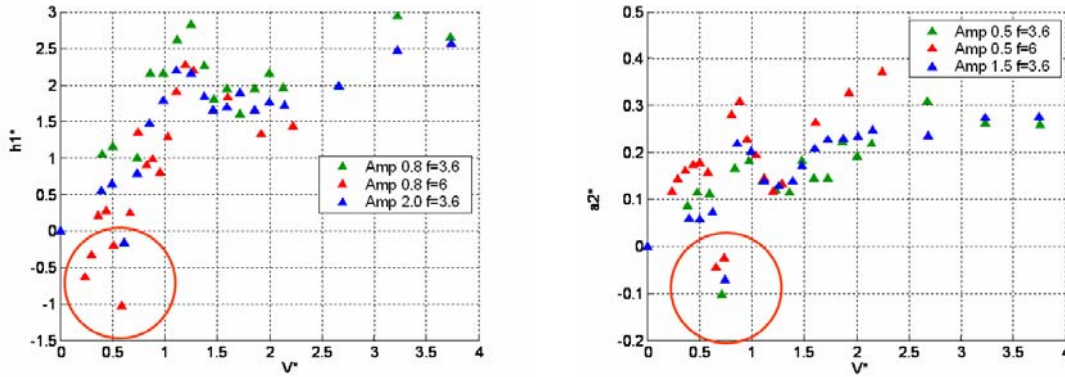


Figure 5. Flutter derivatives h_1^* and a_2^* , at low reduced velocity, expressed in the alternative approach.

which is here related to the first vibration mode, the total damping is obtained by the superposition of aeroelastic and structural damping components. In order to obtain stability against vortex-shedding, the total damping must be positive:

$$\xi \geq -\frac{\rho V^* B^2 h_1^*}{8m\pi}. \quad (7)$$

In the present case, it states $\xi \geq 0.47 \text{ ‰}$ (with geometrical data of Table 1, $V^* = 0.5$ and $h_1^* \approx -1.1$ (Figure 5)). Of course, this is an approximate procedure, because vortex shedding is a strongly non-linear phenomenon; it is here treated by a linear approach, but this allows to estimate the order of magnitude for the minimum structural damping which is necessary to protect the structure from vortex-shedding.

4. Cable vibration damping

Commonly, in order to mitigate the stay cable vibrations, stiffening systems (such as secondary cables) or damping devices (as, for instance, TMD and visco-elastic dampers) are placed on the cables themselves, normally close to the cable end. When visco-elastic dampers are used, as it usually occurs in the case of large dimension stays, one of the design problem is to determine the optimal value for the damping coefficient. The damping parameter optimization is made by taking into account: (a) the reference mode number; (b) the damper location; (c) the Scruton number. Usually, in-plane dampers are sufficient to solve vibration problems. Nevertheless, due to the high tension level, out of plane cable and damper features can be assumed to be the same as the in-plane ones.

4.1 Cable properties

Stay cables are arranged in groups; each group is composed of four cables (Figure 6a). Table 4 resumes the geometrical and mechanical properties of cables, the cable tension due to permanent loads, the dynamic parameters and the minimum value of damping ratios which is necessary to avoid aeroelastic phenomena. Cable frequencies correspond to straight cables first mode; $\xi_{Sc=10}$ and ξ_{gall} are the minimum damping ratios based, respectively, on the Scruton number and the galloping criteria, as described in the next paragraph.

Table 4. Geometric, dynamic and mechanical properties, forces and minimum damping ratios of single cables.

Cable group	L [m]	α [deg]	ϕ [mm]	A_{nom} [cm ²]	E [MPa]	w [kg/m]	N_{perm} [kN]	f_1 [Hz]	$\xi_{Sc=10}$ [%]	ξ_{gall} [%]
1	162	29.6	142	138	1.63e+05	108.3	7847	0.83	0.23	0.39
2	137	34.3	128	112	1.63e+05	87.9	6017	0.96	0.23	0.38
3	113	41.1	118	95.5	1.63e+05	75.0	5173	1.17	0.23	0.34
4	90	51.3	111	83.2	1.63e+05	65.3	4890	1.52	0.24	0.28
5	73	67.3	92	57.1	1.63e+05	44.8	3743	1.99	0.24	0.26

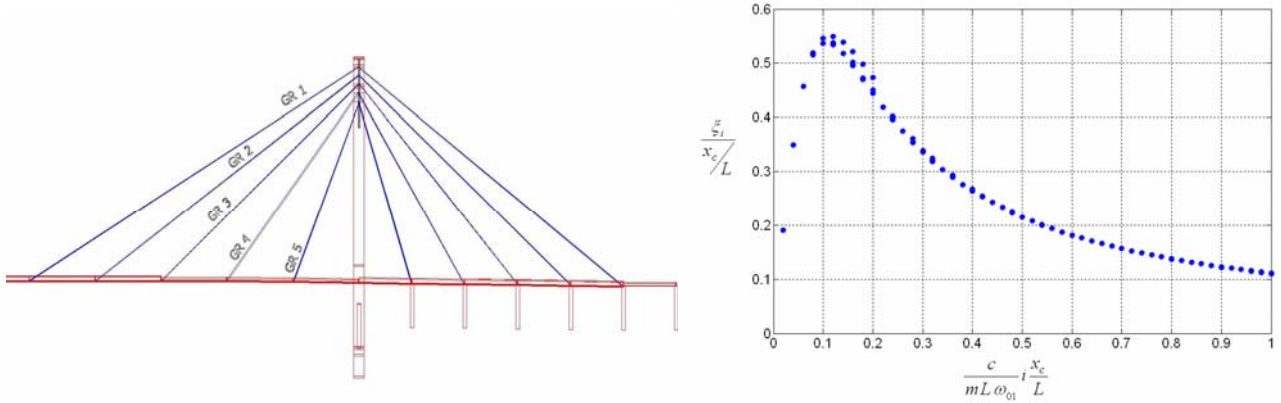


Figure 6. (a) Cable groups arrangements; (b) Pacheco's universal dimensionless damping curve.

4.2 Design criteria

The existence of an optimal value for the damping coefficient was demonstrated by Kovacs (1982). In fact, increasing damping over a certain threshold can induce a fictitious stiffness in the cable which vanishes the energy dissipation role of the damper. The concept can be clearly understood by considering the limit conditions $c=0$ e $c=\infty$. Of course, if $c \rightarrow 0$, the damping capacity tends to be null; on the other hand, if $c \rightarrow \infty$, the damper behaves as a rigid restraint at the location point and the cable simply changes its modal frequencies and shapes, without any energy dissipation.

Pacheco et al. [4] demonstrated the existence of a universal damping curve (Figure 6b) which relates the cable/damper parameters to the effective damping ratio added by the damping system. Following the Pacheco's formulation, the damping coefficient to optimize the damping ratio for a given cable vibration mode is:

$$c_{opt,i} = \frac{0.1 \cdot m \cdot L \cdot \omega_{01}}{i \cdot \frac{x_c}{L}} \quad (8)$$

where $c_{opt,i}$ is the required optimal damping coefficient, m is the cable mass per unit length, L is the cable length, ω_{01} is the circular frequency of the first vibration mode of the undamped cable, x_c is the damper location distance from the cable end anchorage, i is the reference mode number for the optimization.

Figure 6b shows that, for a given damper and cable, the damping ratio depends on the mode number (i) and on the damped location (x_c / L). In the present case, x_c / L is determined by the architectural design condition $h_c = 1.5 m$ (h_c being the - constant - level of the damper-cable connection with respect to the cable lower anchorage) and the optimization has been calibrated on the 2nd mode ($i = 2$), so that an adequate damping level is guaranteed for, at least, the first 6÷8 modes.

In order to evaluate the minimum required damping ratio, two basic criteria have been considered. Firstly, the cable galloping (due to the possible presence of ice) has to be avoided. Based on the Eurocode 1 (EN 1991-1-4:2005), paragraph E.2.2 suggested criteria, the minimum damping ratio (ξ_{gall} in Table 4) is determined by imposing that the galloping onset wind velocity (v_{CG}) satisfies the condition: $v_{CG} > 1.25 v_m$, where $v_m = 40$ m/s is the design mean wind velocity at the cable midspan.

In addition, other aeroelastic phenomena (such as the rain wind induced vibration, the 3D vortex shedding, etc.) have to be avoided and frequent vibrations (due, for instance, to the vortex shedding and to the parametric excitation induced by the supports - deck and towers - movement) have to be mitigated, to reduce the probability of fatigue failure in the cables. Despite no consolidated criteria are available at these purposes, Irvin (1997) observed that whenever the Scruton number

$$Sc = \frac{m \xi}{\rho \phi^2} \quad (9)$$

is higher than 10, as order of magnitude, the cited requirements are practically satisfied. In Eq. (9), m is the cable mass

per unit length, ρ is the air density, ϕ is the cable diameter and ξ is the damping ratio. Different international standard codes have adopted this empirical criterion; subsequently, the reference damping ratio $\xi_{Sc=10}$ in Table 4 is evaluated by placing $Sc \geq 10$ in Eq. (9).

4.3 Dampers requirement and performance

The damping design properties have been determined by following the Pacheco's optimization criterion and by imposing that the minimum damping ratios, as outlined in the Table 4, will be largely satisfied for the first 8 modes. In Table 5, the damping coefficients and the subsequent dampers performance are resumed. The dampers requirement are also reported, in terms of maximum displacement, velocity, force and dissipating power. They have been evaluated under the hypothesis that the first mode is dominant and the maximum oscillation amplitude at the cable midspan, is the same order of magnitude as the cable diameter. This hypothesis is described by the literature to be safety side, based on numerous field observations. Quantities reported in Table 5 represent, respectively: x_c / L , the distance of the damper-cable connection from the lower cable anchorage, with respect to the cable length (based on $h_c = 1.5$ m); c , the damper coefficient, determined as the (Pacheco's) optimal value for the 2nd mode; ξ_2 , ξ_1 , ξ_8 , the damping ratios relative to the modes 2 (optimal) 1 and 8 (limits of the monitored modes); Sc_1 , the Scruton number relative to the 1st mode; $D_{max,Xc}$, $V_{max,Xc}$, $F_{max,Xc}$, the maximum amplitude of the expected damper displacement, velocity and force (based on the above cited hypothesis); P_{max} , the subsequent maximum power which the dampers have to dissipate.

Table 5. Dampers requirement and performance.

Cable group	x_c / L	c [kNs/m]	ξ_1 [%]	ξ_2 [%]	ξ_8 [%]	Sc_1	$D_{max,Xc}$ [mm]	$V_{max,Xc}$ [mm / s]	$F_{max,Xc}$ [kN]	P_{max} [W]
1	0.0187	244	0.75	0.97	0.47	32.2	8.4	44	10.7	232
2	0.0195	185	0.78	1.01	0.49	33.5	7.8	47	8.7	206
3	0.0203	153	0.81	1.05	0.51	34.9	7.5	55	8.4	231
4	0.0214	131	0.86	1.11	0.54	36.3	7.5	71	9.4	335
5	0.0224	91	0.89	1.16	0.56	37.9	6.5	81	7.3	296

5. Conclusions

In the present paper, two of the main experiences related to the design of a cable stayed bridge (across the Adige River) have been reported: the aeroelastic excitation of the bridge deck and the cable vibration mitigation.

The first one is essentially based on aeroelastic tests carried out at the Politecnico of Milano wind tunnel on a 1:30 scaled deck model, in which the aeroelastic derivatives have been determined. The flutter critical conditions (velocity and frequency) have been determined by mean of the Scanlan-Tomko procedure and compared with the simplified Theodorsen theory. The influence of the angle of attack and of the inherent structural damping on the critical parameters has been outlined.

The second one concerns the design of dampers to mitigate the cable vibration. Particular attention has been focused on the criteria adopted to determine an optimal damping coefficient and the dissipation power for the dampers.

6. References

- [1] R.H. SCANLAN, J.J. TOMKO, 1971. "Airfoil and bridge deck flutter", *Journal Engineering Mechanical Division*, Vol. 97, No. 6, 1717-1737.
- [2] DIANA, G., RESTA, F., BELLOLI, M., ROCCHI, D. 2005. "Comportamento aerodinamico del ponte sul fiume Adige". *Final Report*.
- [3] A. ZASSO. "Flutter derivatives advantages of a new representation convention". *J. of Wind Eng. and Ind. Aerodyn.*, 60, pp. 35-47, Elsevier, 1996
- [4] M. PACHECO, Y. FUJINO, A. SULEKH. "Estimation curve for modal damping in stay cables with viscous damper". *Journal of Structural Engineering* 119:6, pp 1961-1979, 1993.